

Supporting Information

Hoogland *et al.* 10.1073/pnas.0809269106

SI Methods

Adenovirus Generation. The G-CaMP2-DsRed sequence was inserted into the transfer vector of the AdEasy kit (JHU-23, American Type Culture Collection). Recombinants of this transfer vector and the AdEasy-1 backbone were screened by using the kanamycin resistance coded on the transfer vector insert. The recombinant plasmid was linearized with PacI (New England BioLabs) and transfected with Transfectin (Bio-Rad) into 293 cells cultured in DMEM (Gibco) with 5% calf serum, 5% FBS and 0.4 mM L-arginine. The virus was harvested 9 days after transfection by freeze/thawing (F/T) the cell pellet in virus suspension buffer containing 150 mM NaCl, 5 mM KCl, 10 mM MgCl₂, 50 mM Tris-HCl, pH7.4. Then the virus was amplified in 293 cells for 44 h postinfection, and again harvested by F/T and

either stored for injections at -80°C or purified by equilibrium centrifugation in a CsCl gradient (1) and dialyzed in saline containing 135 mM NaCl, 5.4 mM KCl, 1.8 mM CaCl₂, 5 mM MgCl₂, 5 mM Hepes-HCl, pH 7.3. The concentration of infectious particles was 3·10⁸ per mL as determined by counting fluorescent 293 cells 24 h after infection.

Control for Phototoxicity and Tissue Damage. A previously reported increase of the frequency of astrocytic calcium signals during intense illumination raises the possibility that our reported waves are light-induced (2). This was not the case, because the rate of spontaneous waves remained unaltered over the duration of our experiments (Fig. 3D). Waves are unlikely to be an artifact of dye loading during pipette insertion because they occurred in tissue expressing the calcium sensor protein G-CaMP2.

1. Lonberg-Holm K, Philipson L (1969) Early events of virus-cell interaction in an adenovirus system. *J Virol* 4(4):323–338.

2. Wang X, *et al.* (2006) Astrocytic Ca²⁺ signaling evoked by sensory stimulation in vivo. *Nat Neurosci* 9(6):816–823.

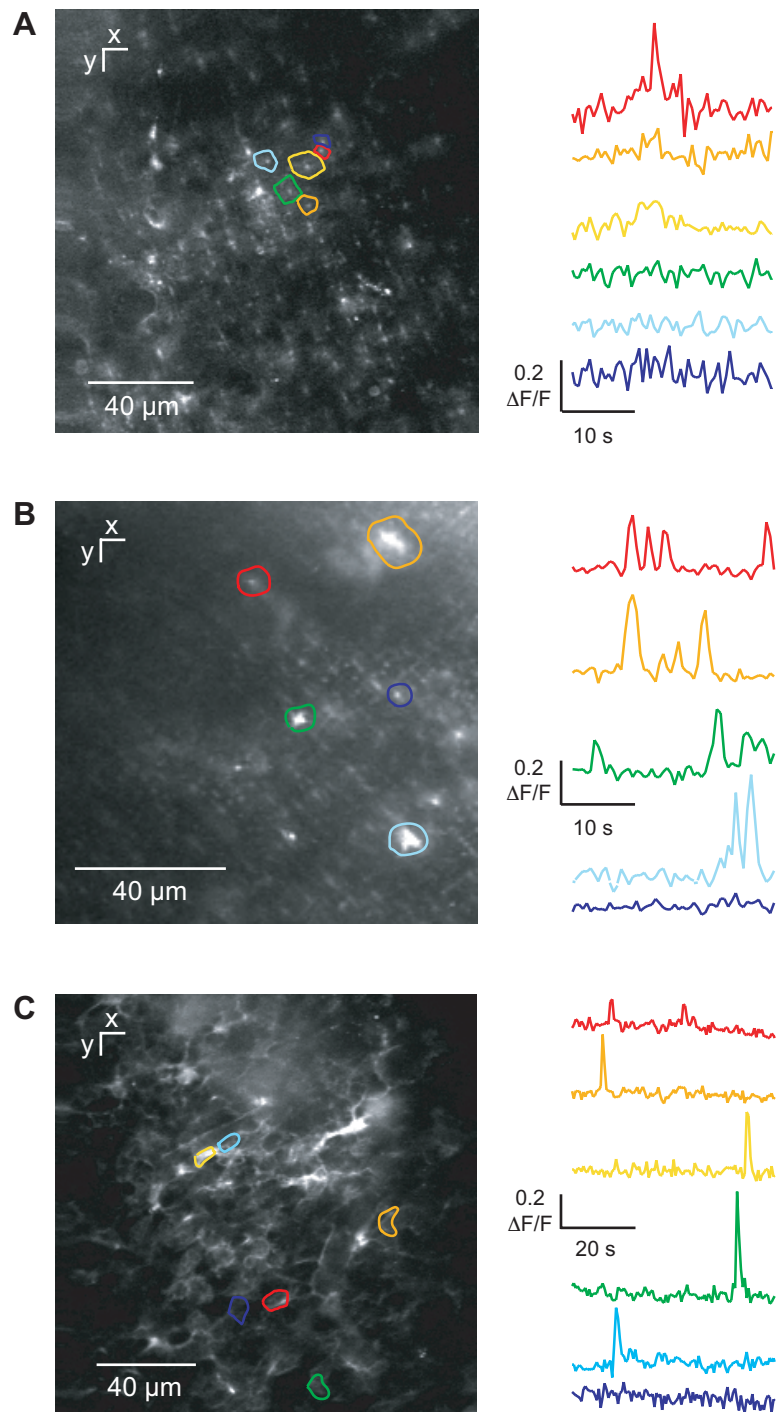
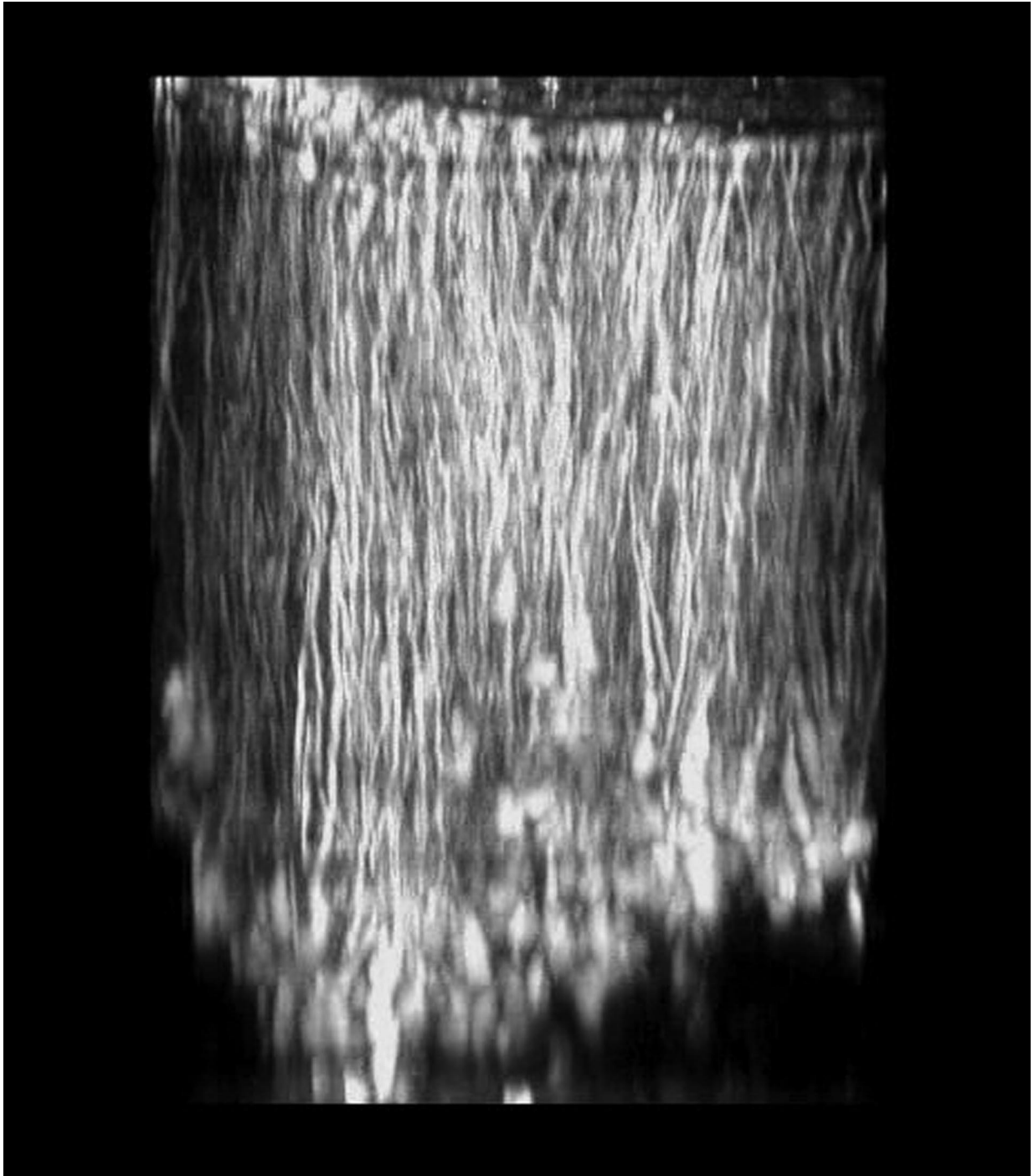
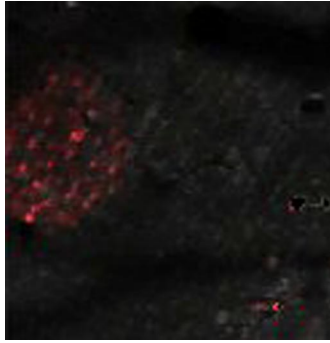


Fig. S1. Subcellular *in vivo* calcium events in BG and velate astrocytes expressing G-CaMP2 in mouse. (A) One BG process is active while the surrounding processes do not participate. (B) Field of view shows higher activity rate in BG processes than in A. (C) Velate astrocyte activity occurs mainly in velate processes (150 μm below pia mater).



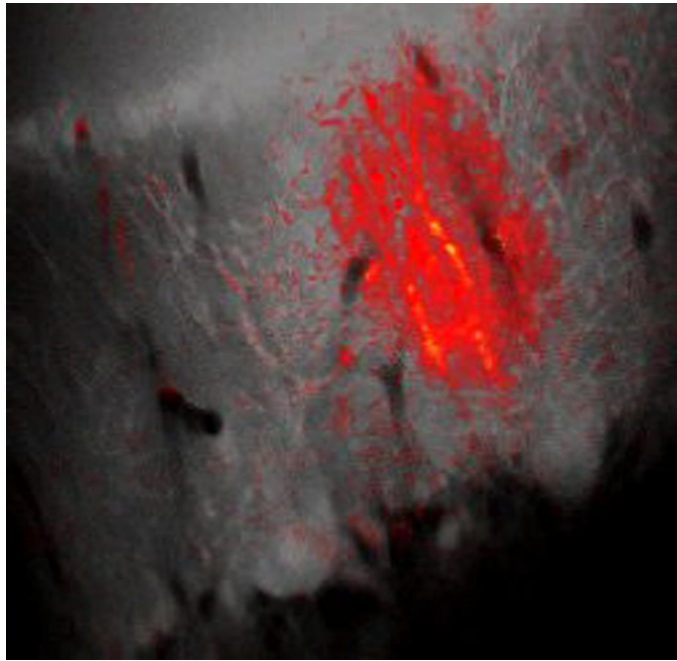
Movie S1. 3D reconstruction of BG expressing GFP under the control of the GFAP promoter in a transgenic mouse. Dimensions of this reconstruction are $130 \times 130 \times 232 \mu\text{m}^3$.

[Movie S1 \(MOV\)](#)



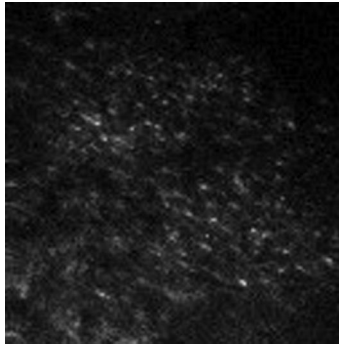
Movie S2. Spontaneous radial expanding calcium wave in the cerebellar molecular layer (*xy*). A radial expanding calcium wave imaged in the superficial molecular layer in a plane parallel to the cerebellar surface. Overlaid color map shows relative fluorescence changes with time (playback is 4 times original speed, diameter of the field of view is 214 μm) with lighter colors indicating larger fluorescence changes. Tissue was bolus-loaded with fluo-5F/AM.

[Movie S2 \(MOV\)](#)



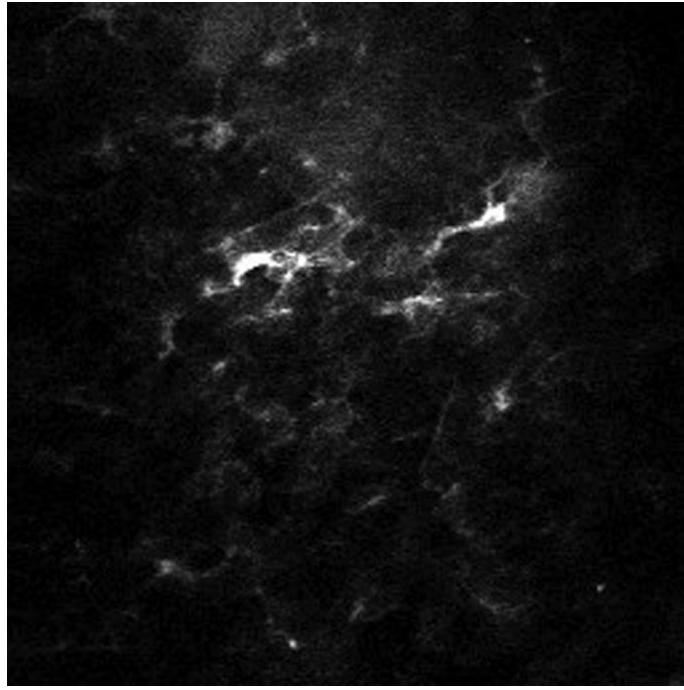
Movie S3. Spontaneous radial expanding calcium wave in the cerebellar molecular layer (xz). A radial expanding calcium wave imaged in a parasagittal plane perpendicular to the cerebellar surface giving a view of the entire cerebellar cortex. Overlaid color map shows relative fluorescence changes with time (playback is 4 times original speed, diameter of the field of view is 195 μm).

[Movie S3 \(MOV\)](#)



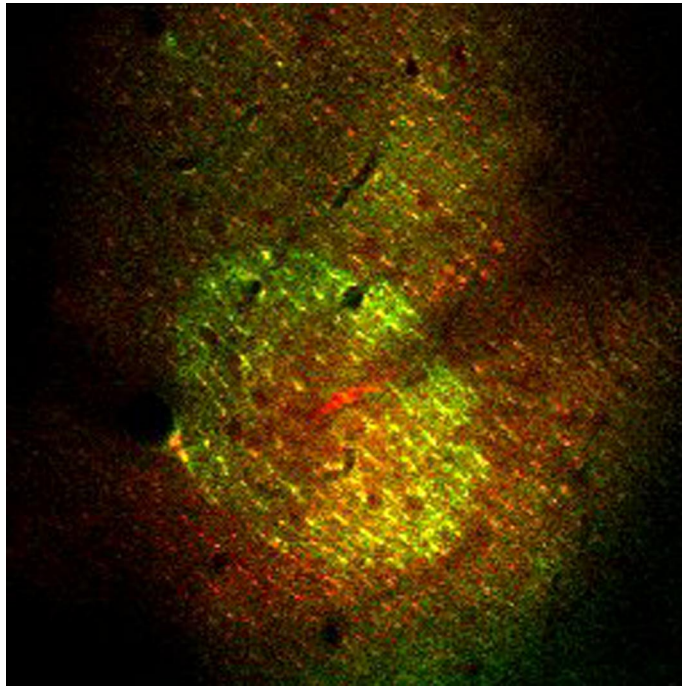
Movie S5. Spontaneous radial expanding calcium waves in the cerebellar molecular layer (*xy*). Raw fluorescence movie of calcium changes reported by G-CaMP2 in the molecular layer of a mouse, showing several ellipsoidal waves in the same field of view (playback is 4 times original speed, diameter of the field of view is 170 μm).

[Movie S5 \(MOV\)](#)



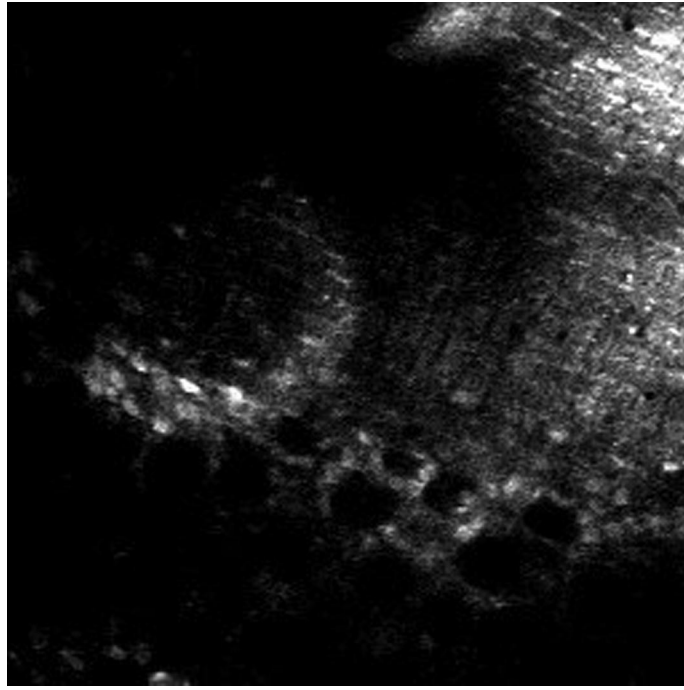
Movie S6. Spontaneous calcium wave in the granule cell layer (*xy*). Raw fluorescence movie of calcium changes reported by G-CaMP2 in the granule cell layer of a mouse (playback is 4 times original speed, diameter of the field of view is 170 μm).

[Movie S6 \(MOV\)](#)



Movie S7. ATP-triggered calcium wave in the cerebellar molecular layer (xy). Green channel displays raw fluorescence reported by fluo-5F; red channels shows Alexa 594 in pipette and during ATP injection as well as SR101 staining of the molecular layer (playback is 4 times original speed, diameter of the field of view is 286 μm).

[Movie S7 \(MOV\)](#)



Movie S8. ATP-triggered calcium wave in the Purkinje cell layer (xy). Raw fluorescence reported by fluo-5F with yellow square indicating time point of ATP ejection. Note the calcium elevations in the somata of Bergmann glia (playback is 4 times original speed, diameter of the field of vision is $286 \mu\text{m}$).

[Movie S8 \(MOV\)](#)

Table S1. Parameters of spontaneous ellipsoidal waves in rat cerebellar cortex

| Spontaneous waves | XY fluo-5F (rat) | XY OGB-1 (rat) | XZ OGB-1 (rat) |
|--|---------------------|-------------------|-------------------|
| No. of events | 85 | 8 | 15 |
| Anesthesia | Isoflurane | Urethane | Urethane |
| Duration, s | 11 ± 5 | 12 ± 4 | 12 ± 4 |
| Expansion time, s | 4.2 ± 2.1 | 3.5 ± 0.8 | 3.5 ± 1.4 |
| Area, μm^2 | 3,500 ± 2,300 | 2,500 ± 1,400 | 3,600 ± 1,500 |
| Major axis, μm | 37 ± 13 | 31 ± 8 | 41 ± 10 |
| Minor axis, μm | 29 ± 12 | 26 ± 8 | 27 ± 6 |
| Major–minor axis ratio | 1.3 ± 0.2 | 1.2 ± 0.3 | 1.5 ± 0.2 |
| Angle to PF, ° | 2 ± 22 | 1 ± 4 | 4.3 ± 12 |
| Speed major axis, $\mu\text{m}/\text{s}$ | 9 ± 5 | 9 ± 3 | 12 ± 5 |
| Speed minor axis, $\mu\text{m}/\text{s}$ | 7 ± 4 | 7 ± 3 | 8 ± 4 |

Table S2. Parameters of spontaneous ellipsoidal waves in mouse cerebellar cortex

| Spontaneous waves | XY G-CaMP2 (mouse) | XY G-CaMP2 (mouse) | XY G-CaMP2 (mouse) |
|--|-----------------------|--------------------|-----------------------|
| No. of events | 10 | 6 | 7 |
| Anesthesia | Urethane | Ketamine/Xylazine | Isoflurane |
| Duration, s | 6.1 ± 1.4 | 4.6 ± 0.6 | 5.9 ± 1.4 |
| Expansion time, s | 2.9 ± 0.6 | 2.2 ± 0.3 | 2.8 ± 0.7 |
| Area, μm^2 | 1,330 ± 450 | 1,510 ± 480 | 1,880 ± 660 |
| Major axis, μm | 30 ± 12 | 22 ± 15 | 34 ± 10 |
| Minor axis, μm | 22 ± 9 | 16 ± 10 | 28 ± 9 |
| Major–minor axis ratio | 1.4 ± 0.2 | 1.3 ± 0.2 | 1.2 ± 0.1 |
| Angle to PF, ° | 7 ± 15 | 8 ± 21 | 6 ± 19 |
| Speed major axis, $\mu\text{m}/\text{s}$ | 22 ± 5 | 25 ± 2 | 24 ± 4 |
| Speed minor axis, $\mu\text{m}/\text{s}$ | 17 ± 4 | 19 ± 2 | 19 ± 3 |

Table S3. Parameters of ATP-triggered ellipsoidal waves in cerebellar cortex

| ATP-triggered $x-y$ | Fluo-5F (rat) | Fluo-5F (mouse) | G-CaMP2 (mouse) |
|-----------------------------------|--------------------|--------------------|--------------------|
| No. of events | 9 | 4 | 9 |
| Anesthesia | Isoflurane | Isoflurane | Isoflurane |
| Duration, s | 7 ± 1 | 8 ± 1 | 7 ± 2 |
| Expansion time, s | 2.9 ± 0.9 | 4.2 ± 0.5 | 3.9 ± 1.0 |
| Area, μm^2 | $19,000 \pm 8,000$ | $16,000 \pm 2,300$ | $14,000 \pm 4,500$ |
| Major axis, μm | 90 ± 20 | 79 ± 2 | 76 ± 12 |
| Minor axis, μm | 63 ± 12 | 65 ± 8 | 59 ± 11 |
| Major-minor axis ratio | 1.4 ± 0.1 | 1.2 ± 0.1 | 1.3 ± 0.1 |
| Angle to PF, $^\circ$ | 0 ± 9 | 2 ± 7 | 2 ± 6 |
| Speed major axis, $\mu\text{m/s}$ | 31 ± 12 | 19 ± 2 | 19 ± 6 |
| Speed minor axis, $\mu\text{m/s}$ | 22 ± 8 | 15 ± 3 | 15 ± 5 |